v. 2, n. 2, 2022

Journal of
Engineering
Research

ESTIMATION OF ABSOLUTE PERMEABILITY IN MICROCT IMAGES OF HIGHLY HETEROGENEOUS CARBONATE ROCKS

Ingrid Bertin Carneiro
Dept. de Engenharia Mecânica, Universidade Federal de Santa Catarina (UFSC)
Campus Universitário Reitor João David Ferreira Lina, Trindade, Florianópolis
Santa Catarina, Brasil
https://orcid.org/0000-0001-7645-826X

Iara Frangiotti Mantovani
Dept. de Engenharia Mecânica, Universidade Federal de Santa Catarina (UFSC)
Campus Universitário Reitor João David Ferreira Lina, Trindade, Florianópolis
Santa Catarina, Brasil
https://orcid.org/0000-0003-4755-0985

Rafael Arenhart
Dept. de Engenharia Mecânica, Universidade Federal de Santa Catarina (UFSC)
Campus Universitário Reitor João David Ferreira Lina, Trindade, Florianópolis
Santa Catarina, Brasil
https://orcid.org/0000-0003-0668-4207

Anderson Camargo Moreira
Dept. de Engenharia Mecânica, Universidade Federal de Santa Catarina (UFSC)
Campus Universitário Reitor João David Ferreira Lina, Trindade, Florianópolis
Santa Catarina, Brasil
https://orcid.org/0000-0003-1229-3616

Celso Peres Fernandes
Dept. de Engenharia Mecânica, Universidade Federal de Santa Catarina (UFSC)
Campus Universitário Reitor João David Ferreira Lina, Trindade, Florianópolis
Santa Catarina, Brasil
https://orcid.org/0000-0001-9815-4398

Francisco Hilário Rego Bezerra
Dept. de Geologia, Universidade Federal do Rio Grande do Norte (UFRN)
Campus Universitário
Natal, Rio Grande do Norte, Brasil
https://orcid.org/0000-0002-0244-0427

Caroline Lessio Cazarin
Centro de Pesquisa e desenvolvimento (CENPES), Petrobras
Cidade Universitária da Universidade Federal do Rio de Janeiro
Rio de Janeiro, Brasil
https://orcid.org/0000-0003-4018-2956

Fábio Luiz Bagni
E&P-Exp, Petrobras
Rio de Janeiro
https://orcid.org/0000-0002-0244-0427

Abstract: Carbonates rocks contain more than 50% of the world's oil prove reserves. Hence, to consider proper strategies in oil recovery methods, the understanding of how fluid flows in such porous media has fundamental importance. Advances in X-ray microCT enable us to retrieve not only most of the details of the internal structure of rocks, but also simulated petrophysical properties. However, one single microCT image can be unable to sufficiently describe the wide range of pore sizes of carbonate rocks, specially the sub-resolution porosity (microporosity). To address this problem, we propose a study to assess the influence of the sub-resolution porosity on the fluid-flow and in the intrinsic permeability values, obtained from carbonate core-plug subsamples microCT images. Brinkman equation is used to model the fluid flow in the entire domain, covering the pores governed by the Stokes equation and the regions of the microporosity governed by Darcy flow (solved using the Finite Volume Method). Simulation results show that when connectivities among the voids are present and microporosity is considered, the value of permeability increases, but remains between the limits, i.e. when consider only the voids and the microporosity as voids. Furthermore, when the pore connectivity place through a microporosity's region, it has an important role to estimate permeabilities.

Keywords: Microporosity, 3D image processing, pore-scale simulation, Brazilian outcrop.

INTRODUCTION

The study of petrophysical properties in porous media is of significance in energy, environmental science and technology. Since carbonates rocks contain more than 50% of the world's oil prove reserves, understanding how the fluid flow through this type of rock is very important to many applications such

as geological sequestration of carbon dioxide, enhanced oil recovery and waterflooding (ISLAM; CHEVALIER; SASSI, 2018). One of the most important petrophysical property is the permeability because it is direct related with the hydrocarbon recovery rate (LUCIA, 1999).

Recent advances in imaging techniques and greater computational resources allow to directly simulate fluid flow into segmented microCT images of rocks and from velocity results to estimate the permeability. This method, which provide insights about properties frequently obtained from expensive and time demanding experiments, is known as digital rock physics and have been gaining room in industry recently (SUN; VEGA; TAO, 2017). However, it has limitations, e. g., the sub-porosity regions cannot be captured at a resolution lower than the resolution of the X-Ray Microtomography. To circumvent this problem, many authors have treated such regions as a combination of void and solid where its distribution depends on the grayscale of this regions (SOULAINE et al., 2016; ABU-AL-SAUD et al., 2020).

In this work, we present a study of the effect of the sub-resolution porosity, categorized here as microporosity, on the fluid flow and consequently, on the permeability estimates. Microporosity can play a significant role in petrophysical properties prediction by connecting clusters of pores and build a continuous path along the sample.

Three-dimensional images of carbonate rocks subsamples that was subjected to the karstification process, were used to simulate the single-phase fluid flow and to evaluate the petrophysical properties. Denoising and edge enhancing filters are applied in the original microCT images, that later are segmented in three regions: voids, solids and microporosity. Then, Brinkman equations are used to model the fluid flow in the entire domain, covering regions of pores (voids) governed by the Stokes equation and regions of the unresolved pores (microporosity) governed by Darcy flow. These equations are solved using the finite volume method implemented in OpenFOAM® (OPENFOAM, 2022).

Besides this introductory section, the present work is subdivided in more three sections. First, we have the section Materials and Methods that includes subsections image acquisition and processing, mathematical model and numerical implementation and simulation setup. Then, the discussion and results are presented to illustrate the effect of microporosity on permeability results. Lastly, we draw the main conclusions.

METHODOLOGY AND METHODS

This section describes all the steps used in this work to obtain the permeability results from microCT images. First, the microCT grayscale image is pre-processed and segmented aiming to determine the three phases of interest: void space, microporosity region and solid phase. Then, the mathematical model and the setup for flow simulations is defined.

IMAGE ACQUISITION AND PROCESSING

We study three different carbonate core-plug subsamples of the Jandaíra Formation, that was subjected the karstification process, gathered from Brazilian state of Rio Grande do Norte. They are imaged using Versa XRM-500 (Zeiss/XRadia) X-Ray Microtomography that provides the three-dimensional (3D) 16-bit grayscale color images. Then, rectangular subvolumes are extracted from such images, whose sizes and voxel size can be seen in Table 1. Figure 1 shows a 3D view in grayscale of the rectangular subvolumes from the samples.

These images are pre-processed via the commercial software Avizo® 8.1 (AVIZO,

MicroCT image	Sample 1	Sample 2	Sample 3
Voxel size (μm)	3.31	8.68	4.62
Subvolume size (voxel^3)	600x500x800	400x400x570	400x500x800

Table 1. MicroCT image information of voxel and subvolume sizes

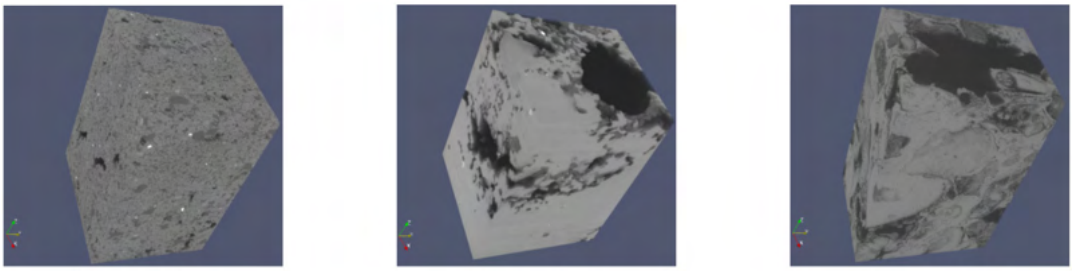

Figure 1. 3D view of the microCT images in grayscale from the samples (a), (b) and (c). The subvolume sizes are shown in Table 1

2022a) applying a Non-Local Means filter (BUADES; COLL; MOREL, 2005) to denoise and an Unsharp Mask (SHEPPARD; SOK; AVERDUNK, 2004) to emphasize texture and details. Then, they are segmented in three phases, void space, rock matrix and microporosity region, using the Watershed segmentation. The Watershed algorithm simulates the progressive immersion of a landscape starting from seed markers of each region. The regions expand according to a priority map (determined by a gradient image) until reaches a watershed line (AVIZO, 2022b).

MATHEMATICAL MODEL

To simulate the single-phase fluid flow through rock samples, we use the Brinkman formulation (BRINKMAN, 1949). Assuming incompressible flow, the continuity and Brinkman equations are stated as:

$$\nabla . \boldsymbol{u} = 0, \tag{1}$$

$$-\nabla p + \frac{\mu}{\varepsilon_{micro}} \Delta \boldsymbol{u} - \frac{\mu}{k_{micro}} \boldsymbol{u} = 0\,, \tag{2}$$

where p is the pressure, μ is the fluid viscosity, $\mathbf{u} = (u_x, u_y, u_z)$ is the velocity, ε_{micro} is the microporosity and k_{micro} is the drag force coefficient, which represents the permeability of the microporous regions, denoted here as micropermeability. This micropermeability is determined using the Kozeny-Carman equation (KOZENY, 1927; CARMAN, 1937):

$$k_{micro} = \frac{d^2}{180} \frac{\varepsilon_{micro}^3}{(1-\varepsilon_{micro})^2}, \tag{3}$$

where d is the characteristic length-scale of the grain-size. As $k_{micro} = f(\varepsilon_{micro})$, therefore k_{micro} varies in range $k_{micro} = 0\ mD$ (impermeable, i.e. solid only) and $k_{micro} = \infty\ mD$ (fully permeable, porous region only). Once that the values of pressure and velocity are obtained, the permeability component in z-direction is written as:

$$k_{zz} = \mu \left(\frac{L_z}{\Delta p}\right) \left(\frac{1}{V} \int_V u_z \, dV\right), \tag{4}$$

where ΔP is the pressure drop, L_z is the sample length in the z-direction, and V is the sample volume.

NUMERICAL IMPLEMENTATION AND SIMULATION SETUP

The Mathematical model composed by eq. (1) and (2) is solved modifying the steady-state solver SimpleFOAM, which is employed to simulate the single phase flow in the porous space, to take into account the Darcy part and the microporosity. The before mentioned solver is available in OpenFOAM, a parallel open-source package for the development of numerical solvers for continuum mechanics problems that employs the finite volume method (ABU-AL-SAUD et al., 2020).

The domain is generated based on the X-ray microtomography segmented images, using the blockMesh and the snappyHexMesh utilities provided by OpenFOAM, considering one cell of the simulation grid as one voxel of the microCT image. After that, the grid is mapped by the microporosity field, ε_{micro}, whose values are linearly interpolated between 0.001 to 1 depending on the grayscale value of the microporosity region. If $\varepsilon_{micro} = 1$, the voxel contains void only, and the flow is governed by the Stokes equation. Values between $0.001 \leq \varepsilon_{micro} < 1$, denote microporous regions whose length is below the voxel size. In these sub-resolution microporous regions, the flow is modeled using Darcy's law.

The simulations were performed on a Workstation with 2 processors Intel(R) Xeon(R) Silver 4114 CPU @ 2.20GHz and 256 GB memory RAM. Convergence is considered achieved when residuals go below 10^{-6}. The relaxation factors α_p and α_u are set to 0.9. The fluid flow parameters used for the simulations are listed in Table 2.

Pressure (Pa)	Kinematic Viscosity (m^2/s)	Density (kg/m^3)
1	10^{-6}	1000

Table 2. Fluid flow parameters

DISCUSSION AND RESULTS

This section presents the simulation results for the three different scenarios regarding to microporosity region: (1) it is assumed as a rock matrix (MProck), (2) it is considered as a map of values normalized from its grayscale values (MPinterpolated) (Fig. 2), and (3) it is considered as a void space (MPvoid). The values of porosity and permeability calculated are shown in Tables 3, 4 and 5.

Figures 3 to 5 show the velocity fields for the three subsamples considering the three scenarios. From these results, the permeability can be obtained using eq.(4), whose values can be seen in Tables 3, 4 and 5. The porosity of the medium presented in the same tables can be calculated using:

$$\varepsilon = \left(\frac{1}{V}\int_V \varepsilon_{micro}\, dV\right). \qquad (5)$$

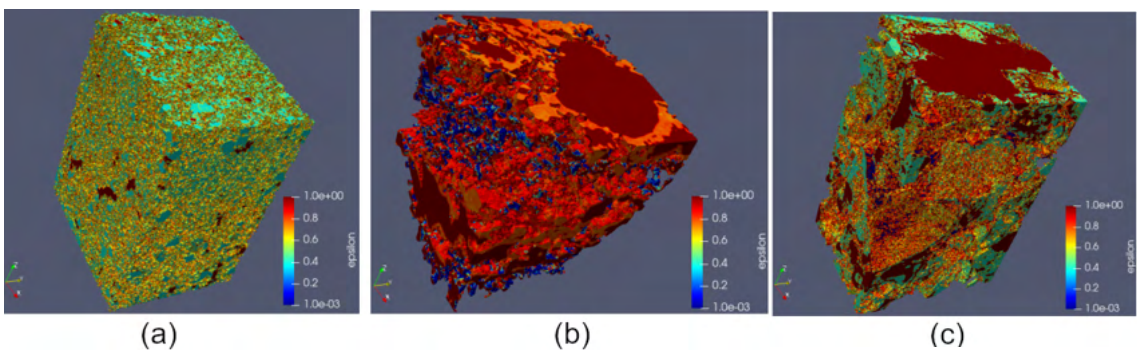

Figure 2. Grid with microporosity values of a) Sample 1, b) Sample 2 and c) Sample 3. Colors indicate the porosity (epsilon - ε) value after the linear interpolation

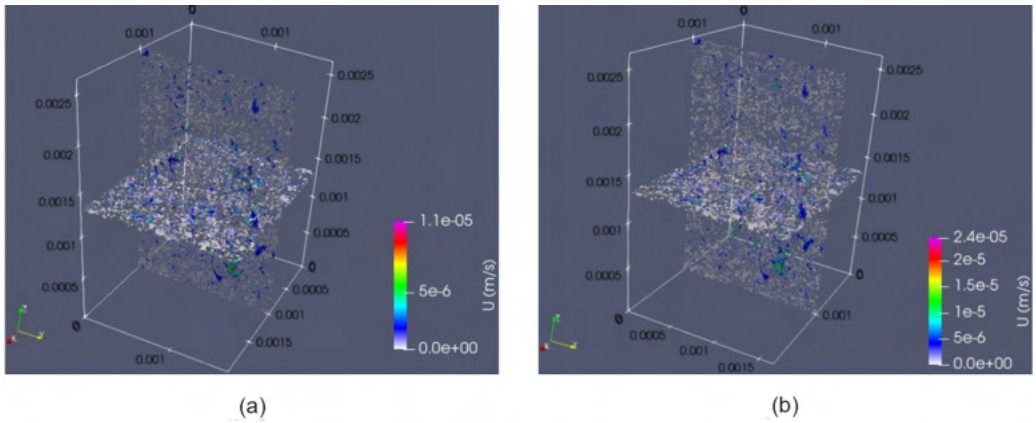

Figure 3. Plot of the velocity (U) field for the Sample 1 considering: (a) MPInterpolated and (b) MPvoid

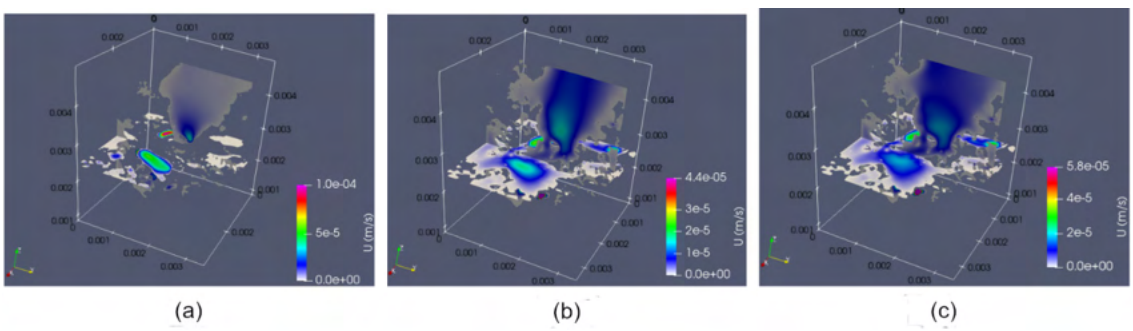

Figure 4. Plot of the velocity (U) field for the Sample 2 considering: (a) MProck and (b) MPinterpolated (c) MPvoid

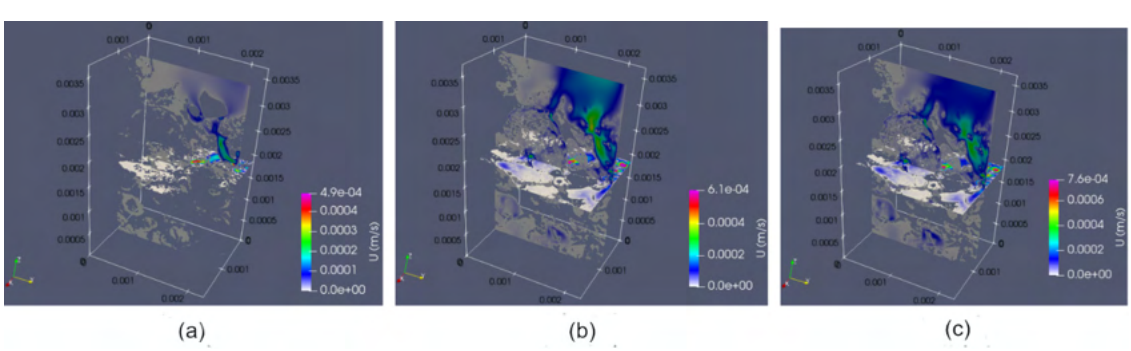

Figure 5. Plot of the velocity (U) field for the Sample 3 considering: (a) MProck and (b) MPinterpolated (c) MPvoid

Sample	Porosity – ε (%)	Permeability – k_{zz} (mD)
Sample 1	6.76	0
Sample 2	20.6	2073.87
Sample 3	31.58	11703.33

Table 3. Values of porosity (ε) and permeability (k) considering MProck calculated for the different carbonate subsamples

Sample	Porosity ε (%)	Microporosity	Permeability k_{zz} (mD)
Sample 1	21.1	14.34	395.19
Sample 2	32	11.4	5632.62
Sample 3	45.16	13.58	11703.33

Table 4. Values of porosity (ε), microporosity and permeability (k) considering MPinterpolated calculated for the different carbonate subsamples

Sample	Porosity – ε (%)	Permeability – k_{zz} (mD)
Sample 1	39	760.7
Sample 2	36.09	8500
Sample 3	60.68	92061.62

Table 5. Values of porosity (ε) and permeability (k) considering MPvoid calculated for the different carbonate subsamples

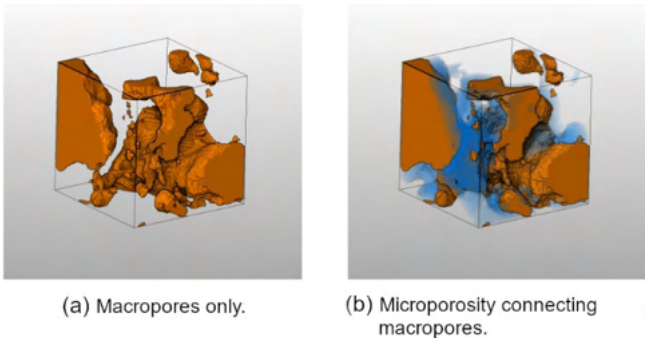

Figure 6. Subsample 50x50x50 of sample 2 showing the microporous (in blue) that serve as a bridge to the macroporous (in yellow)

From the results in the Table 3, 4 and 5 we can observe that the permeability is higher in the third rock sample, and it has the higher porosity and velocity values, showing that this sample has pores larger and more connected compared to the other samples. The sample 1 has the larger percentual of microporosity and percolation does not occur considering only the macropores, showing that the fluid flow only happens with the contribution of microporosity region. In addition, the sample 1 has the microporosity region with pores of smaller size than the others subsamples, resulting in a reduction of the fluid flow, and consequently in a permeability with order of magnitude 10 to 100 times smaller compared to the others.

As expected, when microporosity region is considered as pores (MPvoid), the permeability increase for all samples. Whereas when the microporosity is assumed MProck (Table 3), the three subsamples underestimate the permeability by more than 60%, showing that is important to consider the microporosity regions because they can act as bridges across macropores, as seen in Figure 6, and if they are not considered the results of permeabilities can be underestimated. In future work, we intend to compare the results obtained with experimental data to validate them.

CONCLUSIONS

In this work we study the influence of the sub-resolution porosity (microporosity) on the fluid flow into microCT images of three different carbonate core-plug subsamples of the Jandaíra Formation, that was subjected to the karstification process. The Brinkman formulation is employed to numerically simulate this fluid flow, and from velocity fields, permeability estimates can be obtained using the Darcy's Law. The results show the importance to consider the microporosity regions because since they can act as bridges across macropores, and if they are not considered the results of permeabilities can be underestimates by more than 60% in relation to the results considering the case MPinterpolated. Moreover, for sample 1 fluid flow does not occur if microporosity is disregarded, showing that the fluid flows only through the microporosity region for this sample.

ACKNOWLEDGEMENTS

The authors thank ANP (National Agency of Petroleum, Natural Gas and Biofuels), Petrobras and The Carblab Project for the financial resources during this work.

REFERENCES

ABU-AL-SAUD, M. et al. **Pore-scale simulation of fluid flow in carbonates using micro-ct scan images**. In: INTERNATIONAL PETROLEUM TECHNOLOGY CONFERENCE. International Petroleum Technology Conference, 2020.

AVIZO. **Avizo Software**. Página inicial. Disponível em: https://www.thermofisher.com/br/en/home/electron-microscopy/products/software-em-3d-vis/avizo-software.html. Acesso em: 05 de fev. de 2022.

AVIZO. **Thermo ScientificTM AvizoTM Software 9: Users's Guide**. Disponível em: https://assets.thermofisher.com/TFS-Assets/MSD/Product-Guides/user-guide-avizo-software.pdf. Acesso em: 05 de fev. de 2022.

BRINKMAN, H. **A calculation of the viscous force exerted by a flowing fluid on a dense swarm of particles**. Flow, Turbulence and Combustions, Springer, v. 1, n. 1, p. 27, 1949.

BUADES, A; COLL, B; MOREL, J.-M. **A non-local algorithm for image denoising**. In: 2005 IEEE Computer Society Conference on Computer Vision and Pattern Recognition (CVPR'05), v. 2, p. 60-65, 2005.

CARMAN, P. C. **Fluid flow through granular beds**. Trans. Inst. Chem. Eng., v. 15, p. 150-166, 1937.

ISLAM, A; CHEVALIER, S.; SASSI, M. **Structural characterization and numerical simulations of flow properties of standard and reservoir carbonate rocks using micro-thomography**. Computers & geosciences. Elsevier, v. 113, p. 14-22, 2018.

KOZENY, J. **Uber kapilare leitung der wasser in boden**. Royal Academy of Science, Vienna, Proc. Class I, v. 136, p. 271-306, 1927. Disponível em: https://ci.nii.ac.jp/naid/10029440086/en/.

LUCIA, F. **Carbonate Reservoir Characterization**. Springer, 1999. (Environmental Science). ISBN 9782540637820. Disponível em: https://books.google.com.br/books?id=uZPK4HVsoBkC.

OPENFOAM. **OPENFOAM Software**. Página inicial. Disponível em: https://www.openfoam.com/. Acesso em: 05 de fev. de 2022.

SHEPPARD, A. P.; SOK, R. M.; AVERDUNK, H. **Techniques for image enhancement and segmentation of porous materials**. Physica A: Statistical mechanics and its applications, Elsevier, v. 339, n. 1-2, p. 145-151, 2004.

SOULAINE, C. et al. **The impact of sub-resolution porosity of x-ray microtomography images on the permeability**. Transport in Porous media, Springer, v. 113, n. 1, p. 227-243, 2016.

SUN, H.; VEGA, S.; TAO, G. **Analysis of heterogeneity and permeability anisotropy in carbonate rock samples using digital rock physics**. Journal of Petroleum, Science and Engineering, v. 156, p. 419-429, 2017. ISSN 0920-4105. Disponível em: https://www.sciencedirect.com/science/article/abs/pii/S0920410517305065.